A topological signature in cosmic topology

G.I. Gomero*, M.J. Rebouças†, A.F.F. Teixeira‡,
Centro Brasileiro de Pesquisas Físicas,
Rua Dr. Xavier Sigaud 150,
22290-180 Rio de Janeiro – RJ, Brazil

Abstract

Two procedures for obtaining (extracting and constructing) the topological signature of any multiply connected Robertson-Walker (RW) universe are presented. It is shown through computer-aided simulations that both approaches give rise to the same topological signature for a multiply connected flat RW universe. The strength of these approaches is illustrated by extracting the topological signatures of a flat ($k = 0$), an elliptic ($k = 1$), and a hyperbolic ($k = -1$) multiply connected RW universes. We also show how separated contributions of the covering isometries add up to form the topological signature of a RW flat universe. There emerges from our theoretical results and simulations that the topological signature arises (in the mean) even when there are just a few images for each object. It is also shown that the mean pair separation histogram technique works, and that it is a suitable approach for studying the topological signatures of RW universes as well as the role of non-translational isometries.

*E-mail: german@cbpf.br
†E-mail: reboucas@cbpf.br
‡E-mail: teixeira@cbpf.br

1 Introduction

The astrophysical observations indicate that to a high degree of accuracy our universe is locally homogeneous and isotropic. Thus in the framework of the general relativity theory it can be described through a Robertson-Walker (RW) metric

$$ds^2 = dt^2 - R^2(t)\, d\sigma^2 \,, \tag{1.1}$$

where t is a cosmic time, and $d\sigma^2 = d\chi^2 + f^2(\chi)\,[\, d\theta^2 + \sin^2\theta\, d\phi^2\,]$ with $f(\chi) = \chi\,,\ \sin\chi\,,$ $\sinh\chi\,,$ depending on the sign of the constant spatial curvature ($k = 0, \pm 1$). Clearly $R(t)$ is the scale factor that carries the unit of length.

However, whether we live in a simply or multiply connected space and what is the size and the shape of the universe are open problems, which have received increasing attention over the past few years (see, for example, [1] – [24] and references therein). The most immediate consequence of multiply-connectedness of the universe is the possibility of observing multiple images of cosmic objects, whose existence can be perceived by the simple reasoning presented below.

It is often assumed that the $t = const$ spatial sections M of a RW spacetime manifold are one of the following simply connected spaces: Euclidean E^3 ($k = 0$), elliptic S^3 ($k = 1$), or the hyperbolic H^3 ($k = -1$), depending on the sign of the constant spatial curvature k. However, one can lift the restriction of simply-connectedness for the spatial sections by allowing M to be any one of the possible quotient manifolds $M = \widetilde{M}/\Gamma$, where $\widetilde{M}$ stands for E^3, S^3 or H^3 (depending on the sign of k), and Γ is a discrete subgroup of the full group of isometries of the covering manifold $\widetilde{M}$ acting freely on $\widetilde{M}$ [25]. The action of Γ tesselates $\widetilde{M}$ into identical cells or domains which are copies of what is known as fundamental polyhedron (FP). In forming the quotient manifolds M the essential point is that they are obtained from $\widetilde{M}$ by identifying points which are equivalent under the action of the discrete group Γ. Hence, each point on the quotient manifold M represents all the equivalent points on the covering manifold $\widetilde{M}$. On the other hand, in the general relativity approach to cosmological modelling, the physicists assume that our universe can be modelled by a manifold, and thus a given cosmic object is described by a point $p \in M$, which represents, when M is multiply connected, a set of equivalent points (images of p) on the covering manifold $\widetilde{M}$. So, to figure out that multiple images of an object can indeed be observed if the universe is multiply-connected, consider that the observed universe is a ball $\mathcal{B}_{R_H} \subset \widetilde{M}$ whose radius R_H is the particle horizon, and denote by L the largest

lenght of the fundamental polyhedron P of M ($P \subset \widetilde{M}$). Thus, when $R_H > L/2$, for example, the set of (multiple) images of an given object that lie in $\mathcal{B}_{R_H}$ can in principle be observed. Obviously the observable images of an object constitute a finite subset of the set of all equivalent images of the object.[1]

General relativity (GR) relates the matter content of the universe to its geometry, and reciprocally the geometry constrains the dynamics of the matter content. As GR is a purely metrical (local) theory it cannot be used (without additional topological assumptions as, e.g., asymptotical flatness or asymptotical locally anti-de Sitter [27]) to settle the global structure (topology) of spacetime. One way to tackle the problems regarding the topology of the universe is through a suitable statistical analysis applied to catalogues of discrete cosmic sources to find out whether there are multiple images of cosmic objects, and eventually determine the shape and the size of the universe from the pattern of the repeated images.

Cosmic crystallography [28] (CC) is one of such statistical methods, which looks for distance correlations between the images of cosmic objects using pair separation histograms (PSH), i.e. graphs of the number of pairs of sources versus the distance between them. These correlations arise from the discrete isometries of the covering group Γ, which give rise to the (observed) multiple images. The initial expectation behind the crystallographic method was that these distance correlations would manifest as sharp peaks (called spikes) in PSH's, and that the spike spectrum (their positions and relative amplitudes) would be a definite signature of the topology. The first simulations performed for some specific flat manifolds appeared to confirm these expectations [28] in that the PSH's corresponding to those particular manifolds presented distinct spike spectra. Afterwards, however, histograms were generated for the specific cases of Weeks [29] and one of the Best [30] manifolds and no spikes were found. Their graphs show that, within the degree of accuracy of the corresponding plots, the PSH's of these hyperbolic manifolds exhibit no spikes. However, the spikes in PSH's can either be of topological origin or arise from purely statistical fluctuations. So, it is important to consider that the statistical noise in PSH's can both give rise to sharp peaks of purely statistical origin, and even hide the topological spikes, which are the sharp peaks that really matter in cosmic crystallography. Thus, the ultimate proof (or disproof) for the existence of the topological spikes in a class

[1]For the precise and general condition for the existence of multiple images see [26]. Also note that for $R_H > 2\, r_{inj}$ (here r_{inj} is the injectivity radius, see e.g. [21] for notation) multiple images can still arise.

of manifolds cannot rely only on graphs, since they do not constitute a proof but a clue or simply an indication.[2] As a matter of fact, the proof for the existence of topological spikes ought to arise from a theoretical statistical analysis of the distance correlations to reveal the role in PSH's played by all types of isometries of the covering group Γ.

In considering discrete astrophysical sources in the context of multiply connected RW spacetimes, the *observable universe* is the region or part of the universal covering manifold $\widetilde{M}$ causally connected to an image of a given observer since the moment of matter-radiation decoupling. Clearly in the observable universe one has the set of observable images of the cosmic objects, denoted by $\mathcal{O}$. A catalogue is a particular subset $\mathcal{C} \subset \mathcal{O}$, of *observed* images, since by several observational limitations one can hardly record all the images present in the observable universe. Our observational limitations can be formulated through selection rules which dictate how the subset $\mathcal{C}$ arises from $\mathcal{O}$. Catalogues whose images obey the same well-behaved distribution and that follow the same selection rules are said to be comparable catalogues (for more details about the formalization of these concepts see [26]).

In a recent article, in the context of Robertson-Walker spacetimes, Gomero *et al.* [26] have derived an expression for the expected pair separation histogram (EPSH) for an ensemble of comparable catalogues $\mathcal{C}$ with approximately the same number of sources and corresponding to a manifold M. From the expression for the EPSH they have shown that the spikes of topological nature in PSH's are due to Clifford translations[3] whereas the other non-translational isometries manifest as slight deformations of the EPSH corresponding to the underlying simply connected manifold. This general result holds regardless of the 3-geometry of the spacelike sections of the RW spacetimes, and its restriction to the specific case of Euclidean and hyperbolic 3-geometries gives rise to two basic consequences: (i) that Euclidean manifolds which have the same translations in their covering groups exhibit the same spike spectrum of topological nature; (ii) that individual pair separation histograms (PSH) of hyperbolic 3-manifolds exhibit no spike of topological origin, since there are no Clifford translations in the hyperbolic geometry. From the expression for the EPSH they have found it is also apparent that the contribution due to the multiply-connectedness (topological signature) must arise in PSH's even when there

[2]For preciseness, it should be added that in [29] two causes are presented for the absence of spikes in the simulated PSH corresponding to the Weeks manifold. Note, however, that the explanation in [29] for the lack of spikes in PSH's does not seem to match with those presented in ref. [26].

[3]A Clifford translation is an isometry g of $\widetilde{M}$ such that for all $p \in \widetilde{M}$, the distance $d(p, gp)$ is constant.

are only a few images for each object.[4] These results have been formally derived from very general first principles in [26], nevertheless they have not been thoroughly clarified through concrete simulations.

In the quest for a means of reducing the statistical fluctuations well enough to clear up the signal of non-translational isometries in PSH's, Gomero *et al.* [26] also suggested the mean pair separation histogram (MPSH) as a very first approach to refine upon the crystallographic method. But, although the MPSH procedure rests on a well known result from elementary statistics, apart from the cases recently discussed in [31, 32], no other MPSH has been explicitly built to show that the MPSH scheme is useful in simulations, and that it is a suitable approach for studying the role of non-translational isometries as well as the topological signature of any 3-manifold of constant curvature.

The most patent evidence of multiply-connectedness in PSH's is the presence of topological spikes, which arise when the isometry is a Clifford translation. The other isometries, however, manifest as small deformations of the EPSH corresponding to the underlying simply connected manifold. In computer-aided simulations, however, histograms contain statistical noise, which on the one hand can give rise to sharp peaks of purely statistical origin [33, 26], on the other hand it can mask or even hide the tiny deformations due to non-translational isometries. The most immediate approach to cope with these problems clearly is through the reduction of the noise in PSH's by using, for example, the MPSH scheme. Another possible way of facing them is by focusing in a more appropriate quantity rather than PSH's. Obviously one can also combine these approaches to tackle those problems.

In this article, we firstly recast the theoretical results obtained in [26] to show how one can extract the topological signature of any multiply connected manifold of constant curvature by using a suitable quantity, which turns out to be a constant factor times the difference $\Phi_{exp}(s_i) - \Phi^{sc}_{exp}(s_i)$ of the EPSH corresponding to the multiply connected manifold minus the EPSH of the underlying simply connected covering manifold. Secondly we show, through concrete simulations and based upon our theoretical results, two ways of obtaining (extracting and constructing) the topological signatures of multiply connected manifolds of constant curvature. There also emerges from our theoretical results and simulations how separated contributions of the covering isometries are composed to give

[4]Note however, that whether or not the signatures can be distinguished from the statistical noise when studying a *single* observational catalogue is an independent question.

rise to the (complete) topological signature of a specific manifold. Further, we make clear that the topological signature arises (in the MPSH, i.e. in the mean) even when there are just a few images for each object. Finally, it is also illustrated that the MPSH procedure works by building MPSH's from simulated catalogues, and that it is a suitable approach for studying the topological signature as well as the role of non-translational isometries.

The scope of this paper is as follows. In the next section we set the notation, briefly recast the major result of ref. [26], and presents the theoretical grounds of the two approaches for obtaining (extracting and constructing) the topological signatures of any multiply connected 3-manifolds of constant curvature. In section 3 we present and discuss simulations that make apparent the following issues: (i) that the two procedures for obtaining the topological signature of multiply connected 3-manifolds discussed in section 2 work, and give rise to the same signature; (ii) how the separated contributions of the covering isometries add up to form the plain topological signature of RW universes; and (iii) that the topological signature arises in simulations (in the mean, i.e. through MPSH's) even when there are just a few images for each object. It is also shown in that section that the mean pair separation histogram technique works and that it is a suitable approach for studying the topological signature as well as the role of non-translational covering isometry of any multiply connected 3-manifold of constant curvature (spacelike sections of all RW universes). In section 4 we summarize our main results and briefly indicate possible approaches for further investigations.

2 Topological signature

In this section we shall first set the notation and briefly recast the major result of ref. [26] so as to show how one can extract a topological signature of any multiply connected manifold of constant curvature.

Let us start by recalling that a catalogue $\mathcal{C}$ is a set of *observed* images, subset of the *observable* images, which are clearly contained the observable universe, which in turn is the part of the universal covering manifold $\widetilde{M}$ causally connected to an image of a given observer.

Consider a catalogue $\mathcal{C}$ with n cosmic images and denote by $\eta(s)$ the number of pairs of images whose separation is s. Consider also that our observed universe is a ball of radius a and divide the interval $(0, 2a]$ in m equal subintervals J_i of length $\delta s = 2a/m$.

Each of such subintervals has the form

$$J_i = (s_i - \frac{\delta s}{2}\,,\, s_i + \frac{\delta s}{2}] \qquad ; \qquad i = 1, 2, \ldots, m \ , \tag{2.1}$$

and is centred at

$$s_i = \ (i - \frac{1}{2})\ \delta s \ .$$

The PSH is a normalized function which counts the number of pair of images separated by a distance that lies in the subinterval J_i. Thus the function PSH is given by

$$\Phi(s_i) = \frac{2}{n(n-1)}\ \frac{1}{\delta s}\ \sum_{s \in J_i} \eta(s) \equiv \sum_{s \in J_i} \widehat{\eta}\,(s) \ , \tag{2.2}$$

and is clearly subjected to the normalizing condition

$$\sum_{i=1}^{m} \Phi(s_i)\ \delta s = 1 \ . \tag{2.3}$$

In a multiply connected universe the periodic distribution of images on $\widetilde{M}$ due to the covering group gives rise to correlations in their positions, and these correlations can be couched in terms of correlations in distances between the pairs of images. The examination of the behaviour of these distance correlations can be made as follows.

If one considers an ensemble of comparable catalogues with the same number n of images, and corresponding to the same 3-manifold M of constant curvature, one can compute probabilities and expected values of quantities which depend on the images in the catalogues of the ensemble. Clearly each catalogue of the ensemble gives a set of images distributed in the observed universe. In particular, one can compute the most important quantity for our purpose here, which is the expected number, $\eta_{exp}(s_i)$, of pairs of cosmic images in a catalogue $\mathcal{C}$ of the ensemble with separations in J_i. This quantity is quite relevant because from it one has the expected (normalized) pair separation histogram which clearly is given by

$$\Phi_{exp}(s_i) = \frac{2}{n(n-1)}\ \frac{1}{\delta s}\ \eta_{exp}(s_i) = \frac{1}{N}\ \frac{1}{\delta s}\ \eta_{exp}(s_i) \ , \tag{2.4}$$

where obviously $N = n(n-1)/2$ is the total number of pairs of cosmic images in $\mathcal{C}$, and so the whole coefficient of $\eta_{exp}(s_i)$ is nothing but a normalizing factor.

If one denotes by $F_g(s_i)$ and $F_u(s_i)$, respectively, the probability that the images of a g-pair[5] and an uncorrelated pair be separated by a distance that lies in J_i, the expected

[5]In line with the notation of [26], when referring collectively to correlated pairs we use the terminology Γ-pairs, reserving the name g-pair for a correlated pair corresponding to a specific isometry $g \in \Gamma$. In other words, a g-pair is a pair of the form (p, gp) for any (fixed) isometry g. It should also be noted that the Γ-pairs are the same as the *type II pairs* of Uzan *et al.* [47].

number $\eta_{exp}(s_i)$ can be expressed as

$$\eta_{exp}(s_i) = N_u\, F_u(s_i) + \frac{1}{2} \sum_{g\in\widetilde{\Gamma}} N_g\, F_g(s_i)\ , \tag{2.5}$$

where $\widetilde{\Gamma}$ denotes the covering group Γ without the identity map, and where N_u and N_g denote, respectively, the (total) expected number of uncorrelated pairs and the (total) expected number of g-pairs in a typical catalogue $\mathcal{C}$ of the ensemble.[6]

Inserting eq. (2.5) into eq. (2.4) one obtains

$$\Phi_{exp}(s_i) = \frac{N_u}{N}\ \frac{1}{\delta s}\ F_u(s_i) + \frac{1}{2} \sum_{g\in\widetilde{\Gamma}} \frac{N_g}{N}\ \frac{1}{\delta s}\ F_g(s_i)\ . \tag{2.6}$$

However, from equation (2.4) one is led to define the EPSH's corresponding to uncorrelated pairs and associated to an isometry g, respectively, as

$$\Phi^u_{exp}(s_i) \;=\; \frac{1}{N_u}\frac{1}{\delta s}\ \eta^u_{exp}(s_i) = \frac{1}{\delta s}\, F_u(s_i)\ , \tag{2.7}$$

$$\Phi^g_{exp}(s_i) \;=\; \frac{1}{N_g}\frac{1}{\delta s}\ \eta^g_{exp}(s_i) = \frac{1}{\delta s}\, F_g(s_i)\ , \tag{2.8}$$

where clearly $N_u = \sum_{s_i} \eta^u_{exp}(s_i)$ and $N_g = \sum_{s_i} \eta^g_{exp}(s_i)$.

Thus using (2.7) and (2.8), equation (2.6) reduces to either of the following forms:

$$\Phi_{exp}(s_i) = \mu_u\ \Phi^u_{exp}(s_i) + \sum_{g\in\widetilde{\Gamma}} \mu_g\ \Phi^g_{exp}(s_i) \quad \text{with} \quad \mu_u = \frac{N_u}{N}\,, \quad \mu_g = \frac{1}{2}\,\frac{N_g}{N}\ , \tag{2.9}$$

or equivalently

$$\Phi_{exp}(s_i) = \frac{1}{n-1}\ [\,\nu_u\, \Phi^u_{exp}(s_i) + \sum_{g\in\widetilde{\Gamma}} \nu_g\, \Phi^g_{exp}(s_i)\,] \quad \text{with} \quad \nu_u = 2\,\frac{N_u}{n}\,, \quad \nu_g = \frac{N_g}{n}\ . \tag{2.10}$$

For simply connected manifolds M, since all N pairs are uncorrelated, equation (2.4) reduces to

$$\Phi^{sc}_{exp}(s_i) = \frac{1}{N}\frac{1}{\delta s}\ \eta^{sc}_{exp}(s_i) = \frac{1}{\delta s}\, F_{sc}(s_i)\ , \tag{2.11}$$

where $F_{sc}(s_i)$ is the probability that the two objects in M be separated by a distance that lies in J_i.[7]

Now since the pairs of cosmic images are either correlated (Γ-pairs) or uncorrelated we must have

$$N_u + \frac{1}{2} \sum_{g\in\widetilde{\Gamma}} N_g \;=\; N\ , \tag{2.12}$$

[6]For a formal proof that the decomposition (2.5) can always be made see [26].

[7]It should be noticed that although all pairs in the catalogues corresponding to simply connected manifolds are uncorrelated the probabilities $F_u(s_i)$ and $F_{sc}(s_i)$ are not the same.

which on the one hand leads to

$$\mu_u + \sum_{g \in \widetilde{\Gamma}} \mu_g = 1 \, , \tag{2.13}$$

and on the other hand it gives rise to an alternative expression for the EPSH $\Phi_{exp}(s_i)$ in terms of $\Phi^{sc}_{exp}(s_i)$. Indeed, using (2.9) and (2.13) one easily obtains

$$\Phi_{exp}(s_i) = \Phi^{sc}_{exp}(s_i) + \mu_u \, [\, \Phi^{u}_{exp}(s_i) - \Phi^{sc}_{exp}(s_i) \,] + \sum_{g \in \widetilde{\Gamma}} \mu_g \, [\, \Phi^{g}_{exp}(s_i) - \Phi^{sc}_{exp}(s_i) \,] \, . \tag{2.14}$$

From equation (2.14) one can obtain an expression for the *topological signature* $\varphi^S(s_i) \equiv (n-1)\,[\Phi_{exp}(s_i) - \Phi^{sc}_{exp}(s_i)]$. Indeed, using (2.14) together with the definition of μ_u and μ_g one easily obtains

$$\varphi^S(s_i) = (n-1)\,[\, \Phi_{exp}(s_i) - \Phi^{sc}_{exp}(s_i) \,] = \varphi^U(s_i) + \varphi^\Gamma(s_i) \, , \tag{2.15}$$

where

$$\varphi^U(s_i) = \nu_u \left[\, \Phi^{u}_{exp}(s_i) - \Phi^{sc}_{exp}(s_i) \, \right] \, , \tag{2.16}$$

and

$$\varphi^\Gamma(s_i) = \sum_{g \in \widetilde{\Gamma}} \nu_g \, [\, \Phi^{g}_{exp}(s_i) - \Phi^{sc}_{exp}(s_i) \,] \, , \tag{2.17}$$

and where we have used the definitions of ν_u and ν_g given by (2.10).

An important word of clarification is in order here: although throughout this article we loosely use the terminology topological signature of a manifold and of a universe, it should be stressed that the topological signature $\varphi^S(s_i)$ depends on the pair 3-manifold and observed universe $\mathcal{B}_a$, as well as on the relative position of the FP with respect to $\mathcal{B}_a$.

To show how one can extract through computer-aided simulations the topological signature $\varphi^S(s_i) \equiv (n-1)\,[\Phi_{exp}(s_i) - \Phi^{sc}_{exp}(s_i)]$ of multiply connected universes, a quite important point to be noted is that the EPSH is essentially a typical PSH from which the statistical noise has been withdrawn. Hence we have

$$\Phi(s_i) = \Phi_{exp}(s_i) + \rho(s_i) \, , \tag{2.18}$$

where $\Phi(s_i)$ is a typical PSH constructed from $\mathcal{C}$ and $\rho(s_i)$ represents the statistical fluctuation that arises in the PSH $\Phi(s_i)$. Alternatively from (2.18) one has that a PSH is an EPSH plus the statistical fluctuation.

Using now the decomposition (2.18) together with (2.15) one easily obtains

$$(n-1)\,[\,\Phi(s_i)-\Phi^{sc}(s_i)\,]=\varphi^S(s_i)-\,(n-1)\,[\,\rho(s_i)-\rho^{sc}(s_i)\,]\,, \tag{2.19}$$

where $\rho(s_i)$ and $\rho^{sc}(s_i)$ are the statistical noises which arise in the PSH's corresponding to the multiply connected and the covering manifolds, respectively.

Clearly the right-hand side of (2.19) gives the topological signature $\varphi^S(s_i)$ intermixed with the two statistical fluctuations $\rho(s_i)$ and $\rho^{sc}(s_i)$. In practice, however, one can obviously approach to the suitable quantity $[\Phi_{exp}(s_i)-\Phi^{sc}_{exp}(s_i)]$ by reducing the statistical fluctuations, through any suitable statistical method to lower the noises. The simplest way to accomplish this is to use several comparable catalogues, with approximately equal number of cosmic images, for the construction of a *mean* pair separation histogram (MPSH). For suppose we have K computer-generated catalogues $\mathcal{C}_k$ $(k=1,2,\ldots,K)$ whose PSH's for a given value of m are given by

$$\Phi_k(s_i)=\frac{2}{n_k(n_k-1)}\,\frac{1}{\delta s}\,\sum_{s\in J_i}\eta_k(s)\,, \tag{2.20}$$

where n_k is the number of images in the catalogue $\mathcal{C}_k$. The MPSH defined by

$$<\Phi(s_i)>=\frac{1}{K}\,\sum_{k=1}^{K}\Phi_k(s_i) \tag{2.21}$$

is such that in the limit $K\to\infty$ one has $\Phi_{exp}(s_i)\simeq<\Phi(s_i)>$. Elementary statistics tells us that the statistical fluctuations in the MPSH are reduced by a factor of $1/\sqrt{K}$, which makes clear that MPSH is a suitable approach to deal with the above-mentioned fluctuations.

In brief, the use of the MPSH to extract the topological signature $\varphi^S(s_i)$ consists in the use of K (say) computer-generated comparable catalogues (with approximately the same number n of images and corresponding to the same manifold M) to obtain the mean pair separation histogram $<\Phi(s_i)>$ and analogously to have $<\Phi^{sc}(s_i)>$; and use them as an approximation for $\Phi_{exp}(s_i)$ and $\Phi^{sc}_{exp}(s_i)$, to construct the topological signature $\varphi^S(s_i)\simeq(n-1)\,[<\Phi(s_i)>-<\Phi^{sc}(s_i)>]$. Clearly the greater is the number K of catalogues the lower are the statistical noises $\rho(s_i)$, $\rho^{sc}(s_i)$ and obviously the better are the approximations $<\Phi(s_i)>\simeq\Phi_{exp}(s_i)$ and $<\Phi^{sc}(s_i)>\simeq\Phi^{sc}_{exp}(s_i)$.

An improvement of the above procedure to extract the topological signature $\varphi^S(s_i)$ comes out for the cases one can derive the expression for the PSH's $\Phi^{sc}_{exp}(s_i)$ corresponding to the simply connected covering manifolds. In a recent work [34] (see also [35]) the explicit

formulae for the expected pair separation histogram functions $\Phi^{sc}_{exp}(s_i)$ corresponding to an uniform distribution of objects in the covering manifolds E^3, H^3 and S^3 have been obtained.[8] Thus, for such universes with homogeneous distribution of objects one has from the very beginning $\rho^{sc}(s_i) = 0$, and obviously the topological signature can be rewritten as $\varphi^S(s_i) \simeq (n-1)\,[\,<\Phi(s_i)> - \,\Phi^{sc}_{exp}(s_i)\,]$.

For the sake of selftcontainedness we present below for use in section 4 the explicit expressions for the EPSH's found in refs. [34, 35] corresponding to simply connected Euclidean, hyperbolic and elliptic universes with a uniform distribution of cosmic objects.

Euclidean Universes

$$\Phi^{sc}_{exp}(a,s) = \frac{3}{16\,a^6}\;s^2\,(2a-s)^2\,(s+4a)\;, \tag{2.22}$$

which holds for $s \in (0, 2a]$.

Hyperbolic Universes

$$\Phi^{sc}_{exp}(a,s) = \frac{8\sinh^2 s}{(\sinh 2a - 2a)^2}\;\left[\,\cosh a\;\mathrm{sech}(s/2)\;\sinh(a-s/2)\;\;-\;\;(a-s/2)\,\right]\;, \tag{2.23}$$

which also holds for $s \in (0, 2a]$.

Elliptic Universes

$$\begin{aligned}\Phi^{sc}_{exp}(a,s) \;\;=\;\; \frac{8\sin^2 s}{(2a-\sin 2a)^2}\;\{2a-\sin 2a-\pi+\Theta(2\pi-2a-s)\;\,[\sin 2a\;+\;\pi \\ -\,a-s/2-\cos a\;\;\sec(s/2)\;\;\sin(a-s/2)\;\,]\;\}\;,\end{aligned} \tag{2.24}$$

which holds for all $a \in (0, \pi]$ and $s \in (0, \min(2a, \pi)]$, and where Θ denotes the well-known Heaviside function.

It should be noticed that in (2.24) as well as in (2.22) and (2.23) we have made explicit that the EPSH's depend upon the radius a of the observed universe $\mathcal{B}_a$.

From equations (2.15) – (2.17) it is also clear that another approach to obtain (constructive approach) the topological signature of a multiply connected manifold is by considering the sum of the terms on the right-hand side of (2.15), namely $\varphi^U(s_i) = \nu_u\,[\Phi^u_{exp}(s_i) - \Phi^{sc}_{exp}(s_i)]$ and $\varphi^\Gamma(s_i) = \sum_{g\in\widetilde{\Gamma}}\nu_g\,[\,\Phi^g_{exp}(s_i) - \Phi^{sc}_{exp}(s_i)\,]$. In the next section

[8] Actually, they have found the explicit expressions for the EPSH corresponding to each (Euclidean, hyperbolic and elliptic) observed (homogeneous) universe, which is a spherical ball $\mathcal{B}_a$ with radius a fulfilled with an uniform distribution of cosmic objects.

we shall perform simulations to obtain (construct) the topological signature of a given manifold using also this alternative procedure and make clear that one ends up with the same signature obtainable through the first approach, as it should be expected from the outset. In doing so we will be showing in addition that indeed (2.15), with (2.16) and (2.17), holds within the accuracy of our plot, of course.

To close this section it should be noted that in a recent work, in studying PSH's corresponding to one of the Best manifold, Fagundes and Gausmann [30] have considered the similar quantity $\Phi(s_i) - \Phi^{sc}(s_i)$, instead of the quantity $\Phi_{exp}(s_i) - \Phi^{sc}_{exp}(s_i)$ we are interested here. However, apart from the fact that they have not presented any theoretical argument sustaining their suggestion, from (2.19) one has that their scheme gives rise to a fraction $1/(n-1)$ of the topological signature $\varphi^S(s_i)$ plus (algebraically) the fluctuations corresponding to both PSH's involved, namely that which arises from the multiply connected Best manifold and that originated from the covering space.

3 Topological signature from computer-aided simulations

In this section we shall present and analyze simulations that clarify the following points: (i) how one can obtain (extract and/or construct) the topological signature of multiply connected manifolds; (ii) how separated terms which arise from the covering isometries are composed to form the topological signature of a manifold; and (iii) show that the topological signature arises in simulations (in the mean) even when there are just a few images for each object. In the clarification of theses points we shall use the MPSH technique to make apparent that it is a suitable approach to study the topological signature and the role of non-translational isometries as it has been stated in [26] and illustrated in [31] for the case of flat manifolds.

The first series of computer-aided simulations concerns a compact orientable Euclidean manifold of class $\mathcal{G}_6$ in Wolf's classification [25]. Recently it has been found a set of expressions for the face-pair generators of a fundamental polyhedron (FP) of a cubic manifold of this class. We shall denote this Euclidean manifold by $\mathcal{T}_4$ in agreement with the notation used in [36] and [37], wherein the cubic FP and the pairwise faces identification are shown in figure 1. Relative to a coordinate system whose origin coincides with the center of the FP, the actions of the generators α, β and δ on a generic point $p = (x, y, z)$

were shown to be described by [25, 38]

$$\alpha\, p \;=\; (x+L,\, -y,\, -z)\;, \tag{3.1}$$

$$\beta\, p \;=\; (-x,\, z+L,\, y)\;, \tag{3.2}$$

$$\delta\, p \;=\; (-x,\, z,\, y+L)\;, \tag{3.3}$$

where L is the edge of the cubic FP. Clearly the actions of the inverses of these generators are given by

$$\alpha^{-1}\, p \;=\; (x-L,\, -y,\, -z)\;, \tag{3.4}$$

$$\beta^{-1}\, p \;=\; (-x,\, z,\, y-L)\;, \tag{3.5}$$

$$\delta^{-1}\, p \;=\; (-x,\, z-L,\, y)\;. \tag{3.6}$$

In the simulations corresponding to the cubic manifold $\mathcal{T}_4$ the centre of the FP was taken to be the origin of the coordinate system, and to coincide with the centre of the observed universe $\mathcal{B}_a$, whose diameter $2a$ is such that $2a = L\sqrt{2} \simeq 1.41\, L$. It should be noted that with this ratio for a/L and for $s \in (0, 2a)$ one has only the contribution of non-translational isometries for the topological signature. Indeed, according to eqs. (3.1) – (3.6) the translations of shortest length are due to β^2, δ^2 and their inverses, and are translations of $L\sqrt{2}$ units. So, as we shall take $0 < s < 2a$ no spike will appear in our PSH's for this cubic manifold.[9]

To show how one can extract the topological signature $(n-1)\,[\Phi_{exp}(s_i) - \Phi^{sc}_{exp}(s_i)] = \varphi^S(s_i)$ of $\mathcal{T}_4$, as well as to illustrate the MPSH procedure, and to make clear that the topological signature arises in simulations when there are a few images of some cosmic objects, we have written a program whose input are the number K of catalogues, the radius a of the observed universe $\mathcal{B}_a$, the number m of subinterval (bins), and the number n_s of objects inside the FP (seeds). The program generates K *different* catalogues, starting (each) from the same number n_s of homogeneously distributed seeds inside the FP. For each bin J_i of width $\delta s = 2a/m$ it counts the normalized number of pairs $\sum \widehat{\eta}_k\,(s)$ for all catalogues k from 1 to K. Finally, it calculates the normalized average numbers of

[9]Note, en passant, that the topological signature depends on the pair: 3-manifold and observed universe $\mathcal{B}_a$, and also on the relative position of the FP with respect to observed universe $\mathcal{B}_a$. So, had we considered, for example, a ball with double diameter $4a = 2\sqrt{2} \simeq 2.83$, and kept the same relative position of FP and $\mathcal{B}_a$, the topological signature $\varphi^S(s_i)$ would exhibit spikes at $s = \sqrt{2} \simeq 1.41$, $s = 2$, and $s = \sqrt{6} \simeq 2.45$ and so forth (see ref. [31] for more details).

pairs for all $s_i \in (0, 2a)$, finding therefore, according to (2.21), the mean pair separations histogram $<\Phi(s_i)>$ over K catalogues.

Now, on the one hand we know that the mean pair separation histogram $<\Phi(s_i)>$ is approximately equal to the expected pair separation histogram $\Phi_{exp}(s_i)$ for large enough number K. On the other hand, we have that the explicit expression for $\Phi^{sc}_{exp}(s_i)$ corresponding to a uniform distribution of objects in a Euclidean universe is given by eq. (2.22). Thus, the plot of $(n-1)\,[<\Phi(s_i)> - \Phi^{sc}_{exp}(s_i)\,]$ gives, up to a statistical fluctuation $\rho(s_i)$, a topological signature of the $\mathcal{T}_4$. As a matter of fact, since not all catalogues generated from a fixed number of seeds inside the FP have the same number n of images, in our program instead of n we have used the average number $<n>$ of images per catalogue to plot the topological signature $\varphi^S(s_i)$.

Using the above-described program we have performed simulations for the manifold $\mathcal{T}_4$ with $L = 1$ in an observed universe with radius $a = \sqrt{2}/2 \simeq 0.71$, $\delta s = 0.01$, and with different number n_s of seed objects uniformly distributed in the FP. Figure 1a is the graph of the topological signature $(<n> -1\,)\,[<\Phi(s_i)> - \Phi^{sc}_{exp}(s_i)]$ for the manifold $\mathcal{T}_4$ and was obtained using the MPSH procedure for $K = 16000$ catalogues, and $n_s = 15$, which corresponds to an average number of images per catalogue $<n> \simeq 23$. Figure 1b shows a graph of the topological signature for the same manifold and obtained through the MPSH scheme for identical number of catalogues, but now the number of seeds was taken to be $n_s = 100$, which corresponds to $<n> \simeq 153$ images. These figures clarify the following relevant points: First, that the MPSH approach is indeed a suitable approach to reveal the topological signatures of non-translational isometries; Second, as long as one can extract the topological signature for a small numbers of seeds ($n_s = 15$) and it is essentially the same obtained for a fairly large number of seeds ($n_s = 100$), it becomes clear from these concrete simulations that the plain topological signature arises in simulations where there are just a few images for each object.

According to our earlier discussion, from equation (2.15) – (2.17) it also is clear that an alternative approach to obtain (constructive approach) the topological signature of a multiply-connected manifold is to consider the sum of the terms on the right-hand side of (2.15), namely $\varphi^U(s_i) = \nu_u\,[\Phi^u_{exp}(s_i) - \Phi^{sc}_{exp}(s_i)]$ and $\varphi^\Gamma(s_i) = \sum_{g\in\widetilde{\Gamma}} \nu_g\,[\,\Phi^g_{exp}(s_i) - \Phi^{sc}_{exp}(s_i)\,]$. We have also performed simulations following this approach to determine the topological signature of the manifold $\mathcal{T}_4$ again with $L = 1$ and $a = \sqrt{2}/2 \simeq 0.71$. In doing so we intend, on the one hand, to numerically verify equation (2.15), on the other

hand, to illustrate how the separated terms which arise from the covering isometries sum up to give the topological signature. In what follows we shall report more details of the simulations involved in this second approach.

To make explicit the contribution $\Phi^{g}_{exp}(s_i)$ of a specific isometry $g = \alpha$ (say) to the topological signature term $\varphi^{S}(s_i)$ [see eqs. (2.8) and (2.15) – (2.17)] in computer-generated catalogues we have written a program whose inputs are the total number N_g of correlated pairs, the length L, the radius a of the universe $\mathcal{B}_a$ and the number m of subintervals (bins); and starts by setting a counting variable $k = 0$ and has the following steps:

(i) randomly and homogeneously take an object p (say) inside FP

(ii) apply the isometry α and check if the image αp is still inside the ball $\mathcal{B}_a$. If no, return to step (i), if yes let $k = k + 1$ and go to step

(iii) calculate the distance s between p and αp, then

(iv) call a procedure that computes for all $s \in (0, 2a)$ the normalized sum of pairs $\sum \widehat{\eta}(s)$ whose images are separated by a distance that lies in a bin J_i with width $\delta s = 2a/m$;

(v) check if the k is equal to N_g. If no, return to step (i); otherwise plot the sequence of pairs $[\, x = (j - 1/2)\, \delta s\,,\ y = \sum \widehat{\eta}(s_i)/N_g\,]$ for $j = 1, \ldots, m$ and stop.

We have used this program to compute the contribution of the isometries α and β for $N_g = 16000$, $m = 142$ $(\delta s = 0.01)$, $a = \sqrt{2}/2$ and $L = 1$. Figures 2a and 2b show, respectively, the graphs of $< \Phi^{\alpha}(s_i) >$ and $< \Phi^{\beta}(s_i) >$ for the isometries α and β, whose actions are given, respectively, by (3.1) and (3.2). The fact that the action of isometry α, for example, gives rise to g-pairs whose minimum separation is 1 can be easily understood from the expression for the distance d between p and $\alpha\, p$, namely from $d(p, \alpha p)$. Indeed it is trivial to show that $d(p, \alpha p) \geq 1$. Similarly, form (3.2) one clearly has $d(p, \beta p) \geq \sqrt{2}/2 \simeq 0.71$, making clear that the β-pairs have also a minimum separation.[10]

For the ratio $a/L = \sqrt{2}/2$ and relative position of FP and $\mathcal{B}_a$ that we have chosen, only the isometries given by (3.1) – (3.6) will contribute to the term $\varphi^{\Gamma}(s_i)$. Furthermore, from

[10] Actually, it can be explicitly shown that the set of starting points at which the non-translational isometries begin to contribute for the topological signature are given by $d^2 = 0.5, 1, 4.5, 9, 12.5$, and so forth [31]. Thus, it is clear that the inclusion or exclusion of the contribution of a specific isometry depends on the radius a of the observed universe $\mathcal{B}_a$, reinforcing the fact that the topological signature depends upon the ball $\mathcal{B}_a$.

these equations one clearly has $\Phi^{\alpha^{-1}}_{exp}(s_i) = \Phi^{\alpha}_{exp}(s_i)$ and $\Phi^{\beta^{-1}}_{exp}(s_i) = \Phi^{\beta}_{exp}(s_i)$. Again, due to the symmetry of eqs. (3.1) – (3.6) one easily obtains that $\Phi^{\delta}_{exp}(s_i) = \Phi^{\delta^{-1}}_{exp}(s_i) = \Phi^{\beta}_{exp}(s_i)$. Therefore, the second term on the right hand side of (2.15) reduces to

$$\varphi^{\Gamma}(s_i) \simeq \nu_g \, [\, 2 < \Phi^{\alpha}(s_i) > + 4 < \Phi^{\beta}(s_i) > - 6 \, \Phi^{sc}_{exp}(s_i) \,] \, . \tag{3.7}$$

Finally, for a/L and the relative position of FP and $\mathcal{B}_a$ we have chosen, according to equations (3.1) – (3.6) one easily has that for an uniform distribution of objects the coefficients ν_g are equal for all isometries $g = \alpha, \beta, \delta$ and their inverses. The computation of the value ν_g reduces to the calculation of quotient of volumes, and turns out to be $\nu_g \simeq 0.1161165234$ (for more details on how one can calculate ν_g see [31]). Figure 3 shows the graph of $\Phi^{sc}_{exp}(s_i)$ for $a = \sqrt{2}/2$ as given by (2.22). Figure 4a shows the graphs of this $\varphi^{\Gamma}(s_i)$, given by (3.7), for $\delta = 0.01$, $a = \sqrt{2}/2$ and $L = 1$. It should be stressed that this figure is nothing but the above-described suitable combination of figures 2 and 3 multiplied by the constant factor ν_g .

Again for the same relative position between FP and $\mathcal{B}_a$, the contribution of the term $\varphi^{U}(s_i)$ to the topological signature $[\, \varphi^{S}(s_i) \,]$ of $\mathcal{T}_4$ in shown in figure 4b, and was obtained for the following set of inputs: $m = 142$, $a = \sqrt{2}/2$, $L = 1$, and $K = 16000$.

Figure 5 gives the sum of the contributions due to $\varphi^{\Gamma}(s_i)$ and $\varphi^{U}(s_i)$. The comparison between figures 1a and 1b with figure 5 shows on the one hand that both procedures to obtain the topological signatures work; on the other hand these figures constitute to a certain extent a numerical check for the expression (2.15). Furthermore, figures 2 to 5 also show how the separated terms, which arise from the covering isometries, give rise to the topological signature looked upon as the sum of the terms in the right-hand side of (2.15).

To make explicit that the above procedure employed to extract the topological signature of the Euclidean ($k = 0$) manifold $\mathcal{T}_4$ can be similarly applied to any other classes of 3-manifolds of constant curvature, we have performed computer-aided simulations for an elliptic ($k = 1$) as well as a hyperbolic ($k = -1$) manifolds. In the remainder of this section we shall briefly report the results of our simulations without going into details of the calculations (and programs) for the sake of brevity.

We recall, firstly, that all (locally homogeneous) manifolds with $k = 1$ are known [25], and that they are the simply connected compact covering manifold $\widetilde{M} = S^3$, the (compact) projective space $P^3 = S^3/Z_2$ and the following (compact) quotient manifolds $M = S^3/\Gamma$,

where Γ is one of the following groups: (i) the cyclic group of Z_p of order $p > 2$; (ii) the binary dihedral groups D_r^* of order $4r$ ($r \geq 2$); (iii) the binary polyhedral groups: T^* (where T is the symmetry group of the regular tetrahedron), O^* (where O is the symmetry group of the regular octahedron), and I^* (where I is the symmetry group of the regular icosahedron); (iv) the groups of the form $D_r^* \times Z_p$ with $p \geq 2$ and $r \geq 2$, although for certain values of r, $D_r^* \times Z_p$ can act on S^3 in two different ways; and (v) the groups of the form $H \times Z_p$ ($p \geq 2$), where $H = T^*, O^*, I^*, T_n^*$, and the groups T_n^* are non-cyclic subgroups of T^*.

We have performed computer simulations for the specific elliptic 3-manifold S^3/Z_5, whose volume $2\,\pi^2\,R^3/5$ is one fifth of the volume of S^3. A FP (tetrahedron) together with the pairwise faces identifications is given by Weeks [39]. We have taken as the observed universe the whole covering space S^3, i.e. a solid sphere with radius $a = \pi$ [$R = 1$ in (1.1)]. Thus all catalogues in our simulations for this manifold have the same number of images. Figure 6 shows the graph of the topological signature $\varphi^S(s_i) = (n-1)\,[< \Phi(s_i) > - \Phi_{exp}^{sc}(s_i)\,]$ for a manifold S^3/Z_5 with the edge of the tetrahedron $L \simeq 1.82$ and for $m = 180$, $n = 100$ images ($n_s = 20$), $K = 3000$ catalogues, and where the expression (2.24) for $\Phi_{exp}^{sc}(s_i)$ has been used. Clearly the existence of topological spikes in PSH gives rise to spikes in $\varphi^S(s_i)$. Now since the observed universe is the whole unitary sphere S^3 and the graph of $\varphi^S(s_i)$ shown in figure 6 presents no spike, it becomes apparent that the covering group Γ of this 3-manifold S^3/Z_5 has no translations.

Contrarily to the case of elliptic space-forms a complete classification of the 3-dimensional hyperbolic manifolds has not yet been accomplished. However, from a topological viewpoint the negatively curved (hyperbolic) universes are generic in the sense that most 3-dimensional manifolds can be viewed as homogeneous negatively curved and compact [40]. The volume of the covering manifold H^3 is infinite, but the quotient manifolds H^3/Γ can either be finite of infinite.

We have performed computer simulations for the specific compact hyperbolic 3-manifold known as Seifert-Weber dodecahedral space, which is obtained by identifying or glueing the opposite pentagonal faces of a dodecahedron after a rotation of $3\,\pi/5$. Figure 7 shows the graph of the topological signature $\varphi^S(s_i) = (< n > - 1\,)\,[< \Phi(s_i) > - \Phi_{exp}^{sc}(s_i)]$ for this hyperbolic space where the centre of the dodecahedron was taken to coincide with the centre of the observed universe $\mathcal{B}_a$, whose diameter is $2a = 2.88$. The length L of the edges of the pentagonal faces and the height H of the dodecahedron are such that

$L = H = 1.992769$, where the lengths are measured with the hyperbolic geometry (1.1) with $R = 1$. We have taken $m = 100$ bins, $n_s = 10$ seeds, ($< n > \simeq 18$) $K = 16000$ catalogues, and used the expression (2.23) for $\Phi^{sc}_{exp}(s_i)$. Since the existence of topological spikes in PSH gives rise to spikes in $\varphi^S(s_i)$ and reciprocally, figure 7 also shows that the PSH of even this highly symmetrical hyperbolic manifold presents no topological spikes, clarifying the conjecture made in [30] and in agreement with the results of [26].

It should be stressed that the unit of lengths used in all simulations of this section could certainly have been taken to be of hundreds or thousands of Mpc obviously without changing the patterns of the simulations we have performed. We have avoided large numbers for the sake of simplicity.

To close this section we mention, for the sake of completeness, that small multiply-connected flat models (like those with $\mathcal{T}_4$ topology) may be consistent with COBE CMB constraints (this is still a controversial point, see in this regards, e.g., Levin *et al.* [8], Roukema [41] and Inoue [42]). Nevertheless, according to the current values of the cosmological parameters, a spherical universe is unlikely to be completely observable. Indeed, from the redshift-distance relation for Friedmann-Lemaître-Robertson-Walker with dust and cosmological constant, one can easily obtain that a spherical universe with matter current density parameter $\Omega_{m0} = 0.3$ would require that $\Omega_{\Lambda 0} > 1.35$ for the antipodal point to be visible at a redshift below $z = 1000$, i.e. for S^3 to be inside the sphere representing the microwave background. Similarly with $\Omega_{m0} = 0.3$ would require that $\Omega_{\Lambda 0} > 1.62$ for an antipodal point to be visible at a redshift below $z = 3$, i.e. for S^3 to be coverable by galaxies and quasars. These range of values for $\Omega_{\Lambda 0}$ are in conflict with current constraints on $\Omega_{\Lambda 0}$ and on $\Omega = \Omega_{m0} + \Omega_{\Lambda 0}$ (see, for example, Lange *et al.* [43], Bond *et al.* [44], Balbi *et al.* [45] and Bernardis *et al.* [46]).

4 Concluding Remarks

If we live in a multiply connected Friedmann-Lemaître-Robertson-Walker (FLRW) universe the sky may show multiple correlated images of cosmic objects. The image correlations are dictated by the discrete isometries of the covering group Γ of the 3-manifold used to model its space sections. The periodic distribution of images gives rise to correlations in their positions. In the crystallographic method [28] these correlations are couched in

terms of correlations in distances between the images. Actually, the method of cosmic crystallography (CC) looks for distance correlations between cosmic images using pair separations histograms (PSH), with normalized function given by (2.2), and whose graph gives the (normalized) number of pairs of sources versus the distance between them.

The primary expectations in CC were that the distance correlations would manifest as topological spikes in PSH's, and that the spike spectrum would be a definite signature of the topology. Although the first simulations performed for specific flat manifolds appeared to confirm the initial expectations [28], histograms generated subsequently for hyperbolic manifolds [29, 30] revealed that the PSH's of those manifolds exhibit no spikes. Concomitantly, a theoretical statistical analysis of the distance correlations in the PSH's was performed, and a formal proof was presented that the spikes of topological origin in PSH's are due to translations alone [26]. This result explains the absence of spikes in the PSH's of hyperbolic manifolds, and also gives rise to the fact that Euclidean distinct manifolds which admit the same translations on their covering group present the same topological spike spectrum [26, 31].

Although the set of topological spikes in PSH's is not definite topological signature and is not sufficient for distinguishing even between some compact flat manifolds [31], the most striking evidence of multiply-connectedness in PSH's is indeed the presence of topological spikes, which arise only when the isometry is a Clifford translation. The other isometries, however, manifest as tiny deformations of the expected pair separation histogram (EPSH) corresponding to the underlying simply connected universe. In computer-aided simulations, however, histograms contain statistical fluctuations, which can give rise to sharp peaks of statistical origin, or can hide (or mask) the tiny deformations due to non-translational isometries.

The most immediate approach to cope with fluctuation problems is through the reduction of the noise in PSH's by using the mean pair separation histogram (MPSH) scheme to obtain $<\Phi(s_i)>$ rather than a single PSH $\Phi(s_i)$. However, in most of the computer simulations we have performed, for a reasonable number of images ($n \simeq 60$, or so) and when there is no topological spikes (no translations), the graphs of the $\Phi_{exp}(s_i) \simeq <\Phi(s_i)>$ and $\Phi^{sc}_{exp}(s_i)$ are essentially the same (the deformation of the EPSH due to the non-translational isometries are indeed rather tiny!), making clear that in practice $\Phi_{exp}(s_i)$ is not a suitable quantity for revealing the topology of multiply connected universes.

In this work we have studied two ways of obtaining (extract and construct) the

topological signature of any multiply connected RW universe. The important points in the first approach are: (i) the use of (2.14) to introduce a *new* quantity $\varphi^S(s_i) \equiv (n-1)\left[\Phi_{exp}(s_i) - \Phi^{sc}_{exp}(s_i)\right]$, which turns out to be suitable for revealing the topological signature; (ii) the supplementary use the MPSH technique to drastically reduce the statistical noises and therefore improve the approximations $<\Phi(s_i)> \simeq \Phi_{exp}(s_i)$ and $<\Phi^{sc}(s_i)> \simeq \Phi^{sc}_{exp}(s_i)$.[11]

The second way of obtaining the topological signature of a multiply connected RW universe (constructive approach) is based on the explicit expression for $\varphi(s_i)$ given by (2.15) – (2.17). In this approach the topological signature is obtained by considering the sum of the terms on the right-hand side of (2.15) together with the MPSH technique to reduce the statistical noises.

We have also shown through concrete computer-aided simulations and based upon our theoretical results, that the two ways of obtaining the topological signatures of multiply connected RW manifolds give rise to the same topological signature, as one would have expected from the outset. Furthermore, the strength of these approaches has been shown by extracting the topological signatures of a flat ($k = 0$), an elliptic ($k = 1$), and a hyperbolic ($k = -1$) multiply connected RW universes. There emerges from our theoretical results and simulations that the topological signature arises (in the mean) even when there are just a few images for each object.

It should be emphasized that although in the simulations of section 3 we have assumed that the matter is homogeneously distributed in the universe, the technique we have discussed in this article can be similarly used for other types of matter distribution. In the more realistic cases in which the galaxies (or cluster of galaxies) cluster, the matter distribution is clearly inhomogeneous. This inhomogeneity has been cast in terms of statistical indicators such as correlation functions, which can be used either for the computation of the expression for $\Phi^{sc}_{exp}(s_i)$ or to simulate the clustered distribution of matter in the simply-connected case to have the approximate contribution $\sim \Phi^{sc}_{exp}(s_i)$. Once either of these steps has been carried out one can proceed along the lines described in this paper.

It should be stressed that the ultimate step in most of the statistical approaches to extract the topological signature is the comparison of the signature obtained from

[11] As a matter of fact, although in general necessary, in the present article we did not use the approximation $<\Phi^{sc}(s_i)> \simeq \Phi^{sc}_{exp}(s_i)$, but the explicit expressions for $\Phi^{sc}_{exp}(s_i)$ given by (2.22) – (2.24) for universes fulfilled with an uniform distribution of cosmic objects.

simulated catalogues against similar ones generated from real catalogues. To do so one clearly has to have the simulated patterns of the topological signatures of the manifolds, which can be achieved by the approaches discussed in this paper. Note, however, that the MPSH technique (needed in both approaches) is restricted to simulated catalogues, since it is impossible in practice to have a reasonable ensemble of comparable catalogues of real cosmic sources to calculate mean and expected values of the relevant quantities. An approach to face the important remaining fluctuations problem is to study quantitatively the noise which arises in (2.19) in order to develop suitable filters for those statistical noises which naturally arise in PSH's built from real catalogues.

Note, however, that we have assumed that all cosmic objects of our interest are point-like and have long lifetimes so that none was born or dead since the time corresponding to the redshift cutoff of the catalogue. Moreover, we have also assumed that all objects are comoving, so that their worldlines have constant spatial coordinates. Although simpliflying these assumptions are commonly used in the literature and are very useful to study the observational consequences of a non-trivial topology for the universe.

The main sources of uncertainties of the known statistical approaches to determine the topology of our universe from discrete sources are (see, for example, [26] and [49]):

(i) the cosmological parameters Ω_{m0} and $\Omega_{\Lambda 0}$ are not accurately known or determined, so one cannot accurately compute distances from redshifts. The uncertainty in the determination of the cosmological parameters give rises to uncertainty in the determinations of the positons of the sources, which in turn lead to errors in the determination of distances between pairs of sources.

(ii) the cosmic objects are excactly not comoving, so multiple images are not where they ought to be: in real catalogues there are uncertainties in the positions of the objects due to their peculiar velocities.

(iii) most cosmic objects do not have very long lifetimes, so there may not exist images of the same object at very large different distances from one of our images (observer).

(iv) in most studies of such statistical approaches to cosmic topology the catalogues are taken to be complete. Real catalogues, however, are incomplete: objects are missing due to selection rules, and also most surveys are not full sky coverage surveys.

It should be noticed that if the universe turns out to be small with a covering group

containing Clifford translations, the collecting correlated pairs method (CCP method), which has been recently devised by Uzan, Lehoucq and Luminet [47] (see also [49]), can be used in conjunction with the cosmic crystallographic method to determine both the cosmological parameters Ω_{m0} and $\Omega_{\Lambda 0}$ as well as the topology of the universe. In the remainder of this paper we shall discuss this point in more details.

Instead of grouping the pairs of sources according to their separations to extract the signature of the correlated pairs, in the CCP method one uses the basic feature of the isometries, i.e., that they preserve the distances between pairs of images regardless of whether they are correlated or not. Thus, if (p, q) is a pair of arbitrary images (correlated or not) in a given catalogue $\mathcal{C}$, then for each $g \in \Gamma$ such that the pair (gp, gq) is also in $\mathcal{C}$ we obviously have[12]

$$d(p, q) = d(gp, gq) \; . \tag{4.1}$$

This means that for a given (arbitrary) pair (p, q) of images in $\mathcal{C}$, if there are n isometries $g \in \Gamma$ such that both images gp and gq are still in $\mathcal{C}$, then the distance $d(p, q)$ will occur n times.

The CCP method consists essentially in a count of the number of times each pair distance between images is repeated in a given catalogue.[13] Actually, the CCP-index $\mathcal{R}$ is defined to be the quotient between the result of this count and the total number of pair of sources in $\mathcal{C}$ minus 1 , i.e. $(N - 1)$ in the notation of the second Section.

Now, given that in a catalogue corresponding to a simply connected universe the probability that a given pair separation be repeated is zero, a non-zero CCP-index is an indicator of a non-trivial topology (multiply-connectedness) of our Universe. However, as it has been discussed in [47], the CCP-index $\mathcal{R}$ gives no hint on what is the topology of the spatial sections of the universe.

It should be noticed that cosmic crystallography, its variant approach for simulated catalogues discussed in this work, as well as the CCP method, are them all based on the distance determination between cosmic images, and therefore they are rather sensitive to the (precise) values of the cosmological parameters Ω_{m0} and $\Omega_{\Lambda 0}$. However, as it has been discussed in ref. [47], in a small universe the graph of $\mathcal{R}$ in terms of the cosmological

[12]The pairs for which eq. (4.1) holds have been referred to by Uzan *et al.* [47] as *type I pairs*.

[13]Note that one necessarily has a nonnull CCP-index when there are pattern repetitions in a catalogue $\mathcal{C}$ as that of the scheme used by Roukema [48] in the search for repetition of local quintuplets of quasars in our universe. As he has pointed out his choice for quintuplet rather than any n-tuples was a compromise between the data and computing power available, but the isometries clearly preserve the local n-tuplets.

parameters Ω_{m0} and $\Omega_{\Lambda 0}$ should exhibit a resonance spike at the correct values of these parameters. Therefore, one can use the CCP method to achieve a precise determination of these parameters. So, if the Universe turns out to be (small) Euclidean or spherical, for example, one can use the values of Ω_{m0} and $\Omega_{\Lambda 0}$ determined through the CCP method, and then apply cosmic crystallography (CC) to determine the spike spectrum in the PSH. If the spike spectrum does not uniquely determine the topology of our Universe (as in the case for compact Euclidean manifolds), one can use again the CCP-index in order to distinguish among the possible candidates. Indeed, since the CCP-index is essentially a multiple count of the number of isometries that give rise to repeated distances of images in the observed universe, then the CCP-index corresponding to a given covering group is larger than the one corresponding to any of its subgroups. Therefore, detailed simulations of the CCP method applied to each likely candidate (manifold) can eventually permit to single out one of the possible manifolds (candidates), determining therefore the topology of the universe. This combined method (CCP plus CC and/or its variant approach for simulated catalogues) is currently under investigation, and our results will be shortly published elsewhere.

Captions for the figures

Figure 1. The topological signature $\varphi^S(s_i) = (< n > -1\,)\,[< \Phi(s_i) > - \Phi^{sc}_{exp}(s_i)]$ (obtained through the MPSH technique) of the cubic manifold $\mathcal{T}_4$ with $L = 1$, in an observed universe with radius $a \simeq 0.71$. The horizontal axis gives the pair separation s while the vertical axis furnishes the normalized number of pairs. In (a) the number of seeds is $n_s = 15$ and corresponds to an average number of images per catalogue $< n > \simeq 23$. In (b) the number of seeds is $n_s = 100$ and corresponds to an average number of images per catalogue $< n > \simeq 153$. In both cases one arrives at essentially the same topological signature.

Figure 2. The contribution $\Phi^g(s_i)$ of the isometries $g = \alpha$ [part (a)] and $g = \beta$ [part (b)] to the topological signature $\varphi^S(s_i)$ of the cubic manifold $\mathcal{T}_4$ with $L = 1$ in the observed universe with radius $a \simeq 0.71$. The horizontal axis gives the pair separation s while the vertical axis gives the normalized number of pairs. The MPSH approach was used to obtain both MPSH's $< \Phi^g(s_i) >$. These figures make

clear that the action of the isometries α and β starts, respectively, at $s = 1$ and $s \simeq 0.71$. These starting points for the actions of those isometries give rise to the two discontinuities of the topological signatures $\varphi^S(s_i)$ of figures 1a and 1b.

Figure 3. The EPSH $\Phi^{sc}_{exp}(s_i)$ as given by eq. (2.22) for an Euclidean universe $\mathcal{B}_a$ with radius $a \simeq 0.71$ and fulfilled with an uniform distribution of cosmic objects. The horizontal axis gives the pair separation s while the vertical axis gives the normalized number of pairs.

Figure 4. The contribution of the terms $\varphi^{\Gamma}(s_i)$ [part (a)] and $\varphi^{U}(s_i)$ [part (b)] as given, respectively, by eqs. (2.17) [or (3.7)] and (2.16), to the topological signature $\varphi^S(s_i)$ of the cubic manifold $\mathcal{T}_4$ with $L = 1$ in the observed universe with radius $a \simeq 0.71$. The horizontal axis gives the pair separation s while the vertical axis gives the normalized number of pairs. The exact expression (2.22) was used in part (a) and MPSH technique was used in both part (a) and part (b).

Figure 5. The sum of the contributions due to the terms $\varphi^{\Gamma}(s_i)$ and $\varphi^{U}(s_i)$, given in figure 4, to the topological signature $\varphi^S(s_i)$ [as given by eqs. (2.15) – (2.17)] of the cubic manifold $\mathcal{T}_4$ with $L = 1$ in the observed universe with radius $a \simeq 0.71$. The horizontal axis gives the pair separation s while the vertical axis furnishes the normalized number of pairs. The comparison of this figure with figure 1 shows that the two procedures for obtaining the topological signatures give rise to the same topological signature.

Figure 6. The topological signature $\varphi^S(s_i) = (n-1)\,[<\Phi(s_i)> - \Phi^{sc}_{exp}(s_i)]$ for an elliptic manifold S^3/Z_5 with the edge of the tetrahedron $L \simeq 1.82$. The observed universe was taken to be the whole unitary sphere S^3, and the expression (2.24) for $\Phi^{sc}_{exp}(s_i)$ was used. The horizontal axis gives the pair separation s while the vertical axis gives the normalized number of pairs.

Figure 7. The topological signature $\varphi^S(s_i) = (<n> - 1)\,[<\Phi(s_i)> - \Phi^{sc}_{exp}(s_i)]$ for the Seifert-Weber dodecahedral (hyperbolic) space with $L = H = 1.992769$ (edges L and height H), where the lengths are measured with the hyperbolic geometry (1.1) with $R = 1$. The observed universe $\mathcal{B}_a$ with diameter $2a = 2.88$ was used. The expression (2.23) for $\Phi^{sc}_{exp}(s_i)$ was used. The horizontal axis gives the pair separation s while the vertical axis furnishes the normalized number of pairs.

References

[1] M. Lachièze-Rey & J.-P. Luminet, *Phys. Rep.* **254**, 135 (1995).

[2] J.-P. Luminet, *Past and Future of Cosmic Topology*, gr-qc/9804006 (1998). To appear in Acta Cosmologica, Proceedings of "Concepts de l'Espace en Physique", LesHouches, 29 Sep - 3 Oct 1997.

[3] G.D. Starkman, *Class. Quantum Grav.* **15**, 2529 (1998). See also the other articles in this special issue featuring invited papers from the Topology of the Universe Conference, Cleveland, Ohio, October 1997. Guest editor: Glenn D. Starkman.

[4] N.J. Cornish, D.N. Spergel & G.D. Starkman, *Class. Quantum Grav.* **15**, 2657 (1998).

[5] N.J. Cornish, D.N. Spergel & G.D. Starkman, *Proc. Nat. Acad. Sci.* **95**, 83 (1998).

[6] N.J. Cornish, D.N. Spergel & G.D. Starkman, *Phys. Rev. D* **57**, 5982 (1998).

[7] J.J. Levin, J.D. Barrow & J. Silk, *Phys. Rev. Lett.* **79**, 974 (1997).

[8] J.J. Levin, E. Scannapieco & J. Silk, *Phys. Rev. D* **58**, 103516 (1998).

[9] J.J. Levin, E. Scannapieco & J. Silk, *Class. Quantum Grav.* **15**, 2689 (1998).

[10] J.J. Levin, E Scannapieco, E. Gasperis, J. Silk, & J.D. Barrow *Phys. Rev. D* **58**, 123006 (1999).

[11] D. Stevens, D. Scott & J. Silk, *Phys. Rev. Lett.* **71**, 20 (1993).

[12] J.-P. Uzan, *Phys. Rev. D* **57**, 087301 (1998).

[13] J.-P. Uzan, *Class. Quantum Grav.* **15**, 2711 (1998).

[14] J.R. Weeks, *Class. Quantum Grav.* **15**, 2599 (1998).

[15] N.J. Cornish & J.R. Weeks, *Measuring the Shape of the Universe*, astro-ph/9807311 (1998), to appear as a feature article in the Notices of the American Mathematical Society.

[16] J.R. Bond, D. Pogosyan & T. Souradeep, *Phys. Rev. D* **62**, 043005 (2000).

[17] J.R. Bond, D. Pogosyan & T. Souradeep, *Phys. Rev. D* **62**, 043006(2000).

[18] R. Aurich, *Astrophys. J.* **524**, 497 (1999).

[19] R. Aurich & F. Steiner, *The Cosmic Microwave Background for a Nearly Flat Compact Hyperboli Universe*, astro-ph/0007264.

[20] M.J. Rebouças, R.K. Tavakol & A.F.F. Teixeira, *Gen. Rel. Grav.* **30**, 535 (1998).

[21] J.-P. Luminet & B.F. Roukema, *Topology and the Universe: Theory and Observation*, astro-ph/9901364 (1999). To appear in the Proceedings of Cosmology School held at Cargese, Corsica, August 1998.

[22] V. Blanlœil & B.F. Roukema, Editors of the electronic proceedings of the *Cosmological Topology in Paris 1998*, astro-ph/0010170.

[23] B.F. Roukema, proceedings of review talk at Marcel Grossmann IX Meeting, in press, http://www.icra.it/MG/mg9/mg9.htm, astro-ph/0010189.

[24] J.R. Weeks, proceedings of review talk at Marcel Grossmann IX Meeting, in press, http://www.icra.it/MG/mg9/mg9.htm

[25] J.A. Wolf, *Spaces of Constant Curvature*, fifth ed., Publish or Perish Inc., Delaware (1984).

[26] G.I. Gomero, A.F.F. Teixeira, M.J. Rebouças & A. Bernui, *Spikes in Cosmic Crystallography*, gr-qc/9811038 (1998).

[27] G.J. Galloway, K. Schleich, D.M. Witt, & E. Woolgar, *Phys. Rev. D* **60**, 104039 (1999).

[28] R. Lehoucq, M. Lachièze-Rey & J.-P. Luminet, *Astron. Astrophys.* **313**, 339 (1996).

[29] R. Lehoucq, J.-P. Luminet & J.-P. Uzan, *Astron. Astrophys.* **344**, 735 (1999).

[30] H.V. Fagundes & E. Gausmann, *Cosmic Crystallography in Compact Hyperbolic Universes*, astro-ph/9811368 (1998).

[31] G. Gomero, M.J. Rebouças & A.F.F. Teixeira, *Phys. Lett. A* **275**, 355 (2000).

[32] G. Gomero, M.J. Rebouças & A.F.F. Teixeira, *Int. J. Mod. Phys. D* **9**, 687 (2000).

[33] H.V. Fagundes & E. Gausmann, *Phys. Lett. A* **238**, 235 (1998).

[34] A. Bernui & A.F.F. Teixeira, *Cosmic crystallography: three multi-purpose functions*, astro-ph/9904180 (1999).

[35] M.J. Rebouças, *Int. J. Mod. Phys. D* **9**, 561 (2000).

[36] G.I. Gomero, M.J. Rebouças, A.F.F. Teixeira & A. Bernui, *Int. J. Mod. Phys. A* **15**, 4141 (2000).

[37] A. Bernui, G.I. Gomero, M.J. Rebouças & A.F.F. Teixeira, *Phys. Rev. D* **57**, 4699 (1998).

[38] G.I. Gomero, *Fundamental Polyhedron and Glueing Data for the Sixth Euclidean Compact Orientable 3-manifold*, preprint CBPF-NF-049/97 (1997).

[39] J.R. Weeks, *The Shape of Space*, in the series "Pure and Applied Mathematics," Vol. 96, page 228, Marcel Dekker Inc., New York (1985).

[40] W.P. Thurston, *Three-Dimensional Geometry and Topology*, ed. Silvio Levy, Princeton U. P., Princeton (1997).

[41] B.J. Roukema, *Class. Quantum Grav.* **17**, 3951 (2000).

[42] K.T. Inoue, *COBE Constraints on a Compact Toroidal Low-density Universe*, astro-ph/0011462 (2000).

[43] A.E. Lange *et al.*, *Phys. Rev. D* **63**, 042001 (2001).

[44] J.R. Bond *et al.*, *The Cosmic Background Radiation* circa νK , CITA-2000-63, in Proc. Neutrino 2000 (Elsevier), eds. J. Law and J. Simpson.

[45] A. Balbi *et al.*, *Astrophys. J.* **545**, L1–L4 (2000).

[46] P. de Bernardis *et al.*, *First Results from BOOMERanG Experiment*, astro-ph/0011469 (2000).

[47] J.P. Uzan, R. Lehoucq & J.P. Luminet, *Astron. Astrophys.* **351**, 776 (1999).

[48] B.F. Roukema, *Mon. Not. R. Astron. Soc.* **283**, 1147 (1996).

[49] R. Lehoucq, J.P. Uzan & J.P. Luminet, *Limits of Crystallographic Methods for Detecting Space Topology*, astro-ph/0005515 (2000).

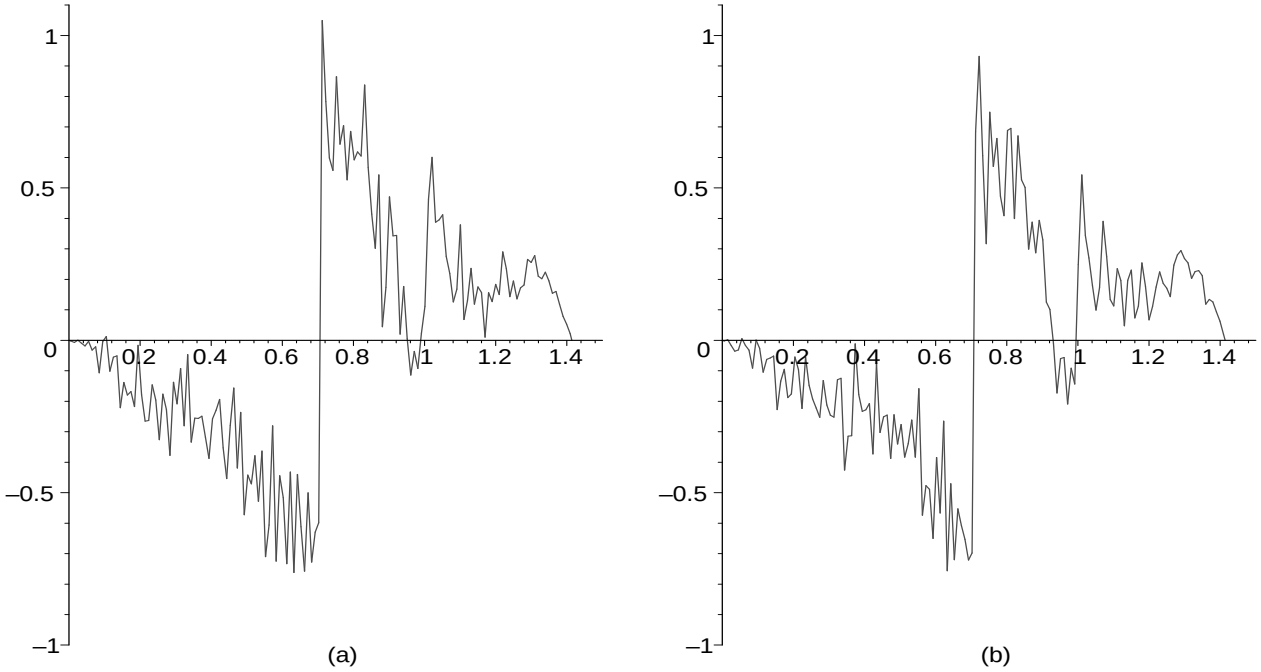

Figure 1

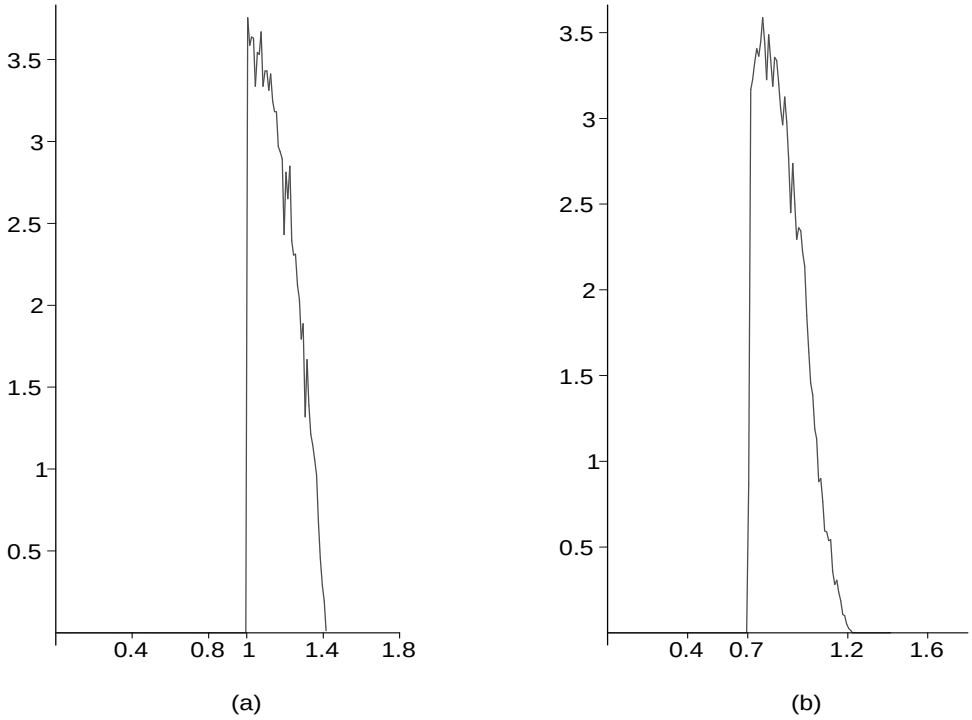

Figure 2

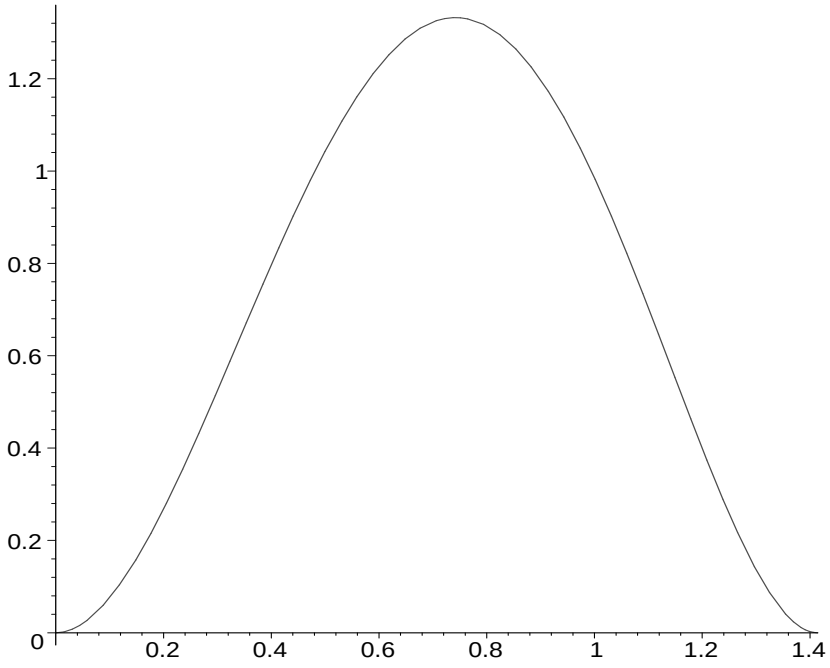

Figure 3

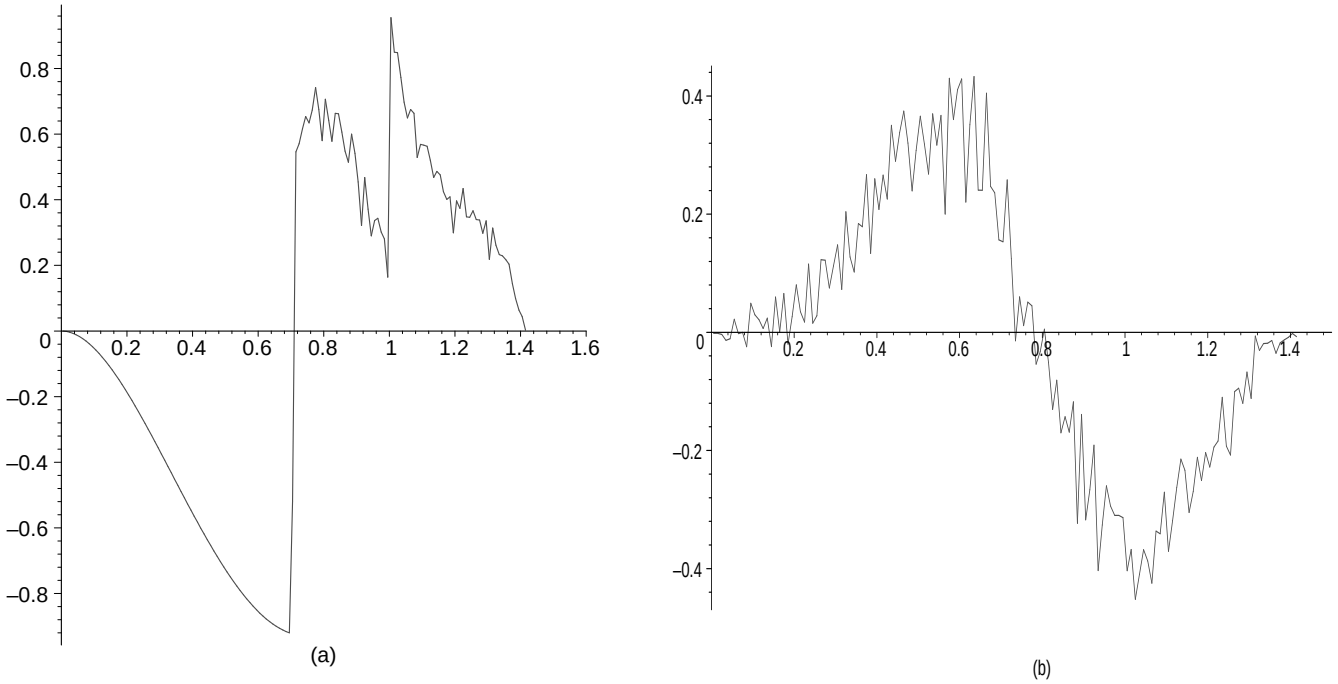
0.8
0.6
0.4
0.2
0
–0.2
–0.4
–0.6
–0.8
0.2
0.4
0.6
0.8
1
1.2
1.4
1.6
(a)
0.4
0.2
0
–0.2
–0.4
0.2
0.4
0.6
0.8
1
1.2
1.4
(b)

Figure 4

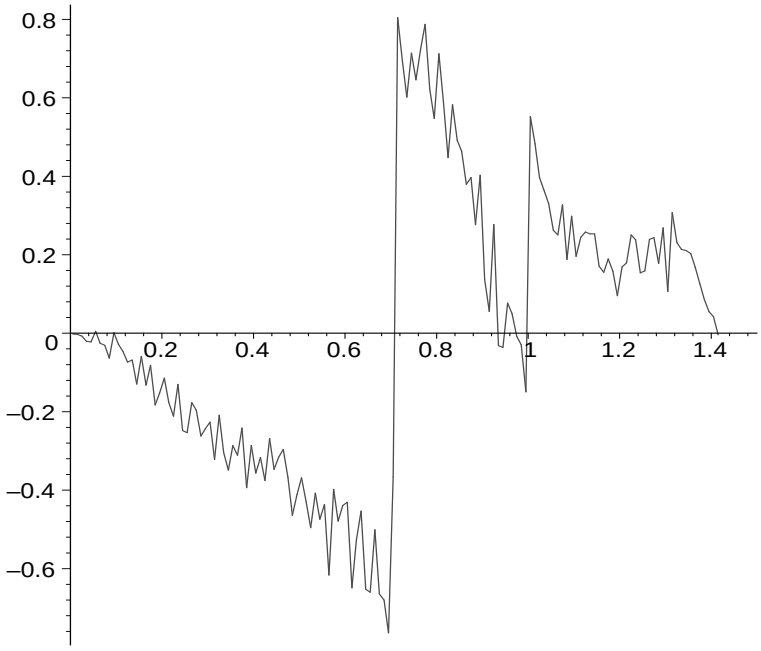

Figure 5

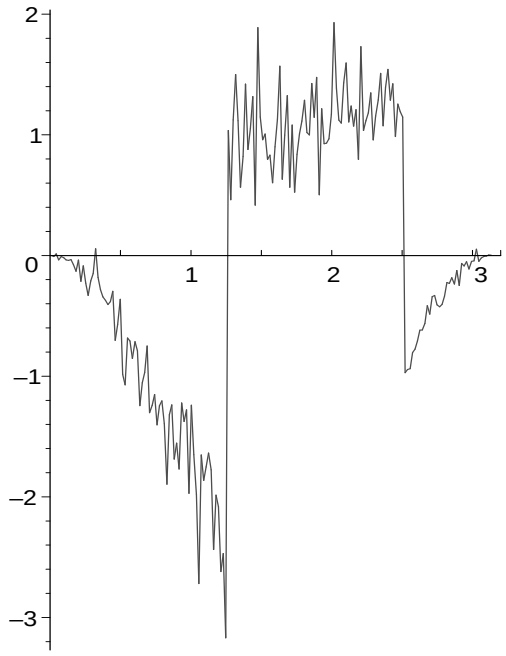

Figure 6

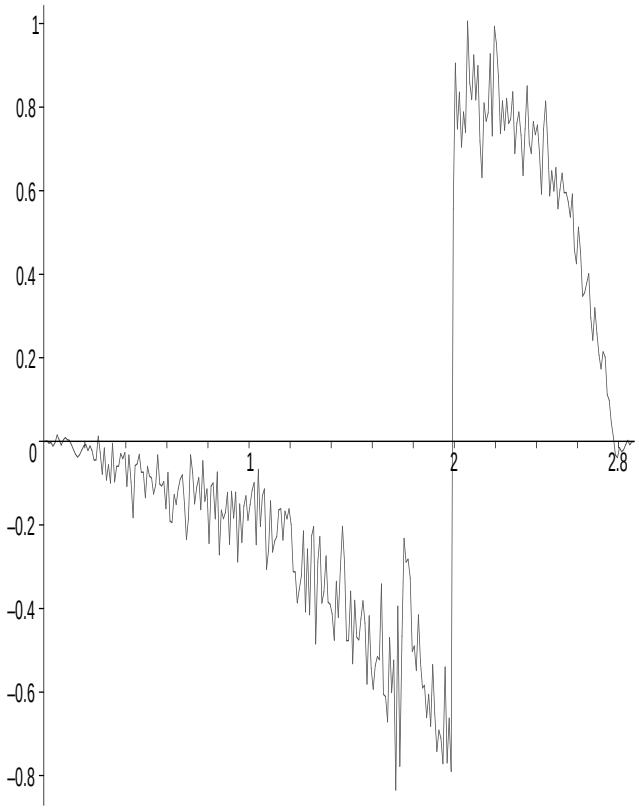

Figure 7